Journal of Intelligent Systems and Internet of Things
Vol. 17, No. 01, PP. 145-158, 2025
DOI: https://doi.org/10.54216/JISIoT.170111

VSG parallel power distribution control strategy by adaptive virtual impedance

Jianfeng Wang[1,2,*], Nurulazlina Ramli[1], Noor Hafizah Abdul Aziz[3]

[1]Centre of Advanced Electrical and Electronic Systems (CAEES), Faculty of Engineering and the Built Environment, SEGi University, Kota Damansara, 47810, Petaling Jaya, Selangor, Malaysia

[2]Faculty of Electrical Engineering, Hebei Vocational University of Technology and Engineering, Xingtai, 054000, China

[3]School of Electrical Engineering, College of Engineering, Universiti Teknologi MARA (UiTM), 40450, Shah Alam, Selangor, Malaysia

Email: ncepu_wjf@163.com; nurulazlina84@gmail.com; noor4083@salam.uitm.edu.my

Abstract

As electric power develops, stable distribution of output power has become a key issue, and more and more power distribution strategies have been proposed. However, most of them are single distribution strategies with large errors and low credibility, which makes it difficult to maintain the stability of motor output distribution power in the actual situation. Therefore, by characteristics of adaptive virtual impedance to reduce small signals influence in the circuit and parallel power stability of virtual synchronous machine virtual synchronous generator control strategy, this research establishes a parallel power model of virtual synchronous generator, selects the changes of voltage and current as the measurement standard of the system, and sets up simulation experiments to determine whether to add adaptive virtual impedance to design a control strategy that can stably distribute output power. Results showed that it can keep output ratio of active power and reactive power within range of 2:1, and voltage difference at the output terminal is 0, and the current is 0.8A, which meets the requirements of circulating current. In a word, the control strategy of virtual synchronous generator designed in this research has high accuracy and strong stability. Compared with previous control strategies, the control strategy of parallel power distribution can ensure the stability of output power in the actual situation. This achievement has certain application prospects in the field of motor power distribution.

Received: December 11, 2024 Revised: February 03, 2025 Accepted: March 01, 2025

Keywords: VSG; Stability; Parallel system; Capacity ratio allocation; Adaptive virtual impedance

1. Introduction

With the slogan of "carbon neutrality and carbon peaking" put forward, people will reduce the use of fossil energy in daily life, thus increasing the use of clean energy to meet daily needs [1]. The emergence of distributed generation

technology enables the natural clean energy to be converted into electric energy for people to use. At this time, the generated electric energy will be connected to the power grid or load using the interface. However, the power supply connected to the power grid system in this way will increase the requirements for grid voltage regulation, frequency modulation, peak shaving and other aspects, and will cause the problem of load power imbalance [2]. Although the above problems have been effectively solved with the development of energy storage technology, the power electronic interface itself has the characteristics of low damping and low inertia, which will be dangerous in the case of large scale distributed generation [3]. The inertia and damping characteristics of a synchronous motor are simulated by the virtual synchronous generator (VSG) system, which makes the energy storage converter have a negative impact on the grid when it is connected to the grid. However, distributed power stations usually have large power, and a single or large capacity PCS will increase the demand for high-quality power devices [4]. Parallel connection of multiple PCSs has become an effective way to solve this problem [5]. Theoretically, it can solve the problems of capacity, large number of systems and fault maintenance, but in reality, the control and distribution of power has become a key problem [6]. In view of the above problems such as unstable circuit control system, difficult output power distribution, and easy overload of power grid, this research attempts to add adaptive virtual impedance (AVI) to parallel power system of virtual synchronous motors to reduce the impact of small signals in the circuit and improve the distribution of output power.

Therefore, this research mainly studies the power distribution control strategy from four aspects. The first part is a summary of the current research status of power distribution mode of circuit system. The second part is to establish the VSG system model for power distribution, implement simulation experiments and analyze the stability. The third part is to add adaptive virtual impedance to the VSG parallel system, optimize the power distribution mode, and analyze the results. The last part is the summary of the whole article.

1. Related works

At present, the increase of system stability caused by adaptive virtual impedance in circuit systems has attracted extensive attention. In the microgrid, the problem of voltage collapse frequently occurs due to insufficient power of distributed generator units during the inverter control circuit. In order to solve this problem of clean energy, Li Z et al. took the photovoltaic output power of solar energy under real conditions as the standard to modify the droop coefficient, and proposed a control strategy that makes droop and virtual impedance adaptive [7]. For VSG that cannot effectively determine the output of reactive power, Liang X and other scholars proposed a method by virtual impedance, which can be applied to grid connection and isolated microgrid [8]. The distributed technology of isolated microgrid has always puzzled scientific researchers with the problems of inaccurate output power distribution and difficulty in determining appropriate value. So researchers like Vijay A S introduced a decentralized technology to adjust virtual impedance in DG controller according to its output current [9]. The stability of the inverter system and the microgrid will negatively influence the circuit output power. Ahmed M et al. proposed an adaptive virtual impedance-based control scheme for the universal voltage source converter (VSC). This scheme aimed to enhance the stability and power sharing performance of the VSC interface in AC/DC hybrid microgrids with varying feeder characteristics and distributed energy. [10]. Adaptive virtual impedance makes it difficult to adjust controller parameters. Wu H and colleagues, using adaptive virtual impedance, created a small signal model of GFM VSCs with current limitation. This was done to guarantee the small signal stability of the system [11]. Renewable energy power generation in the power system continues to improve, and demand for converter based synthetic inertia becomes more important. Babayomi O and fellow scholars achieved distributed secondary regulation of frequency and voltage for the model predictive control voltage source converter in the AC microgrid. The virtual synchronous generator was utilized to simulate inertia and reduce frequency change rates caused by sudden load changes [12]. The angular frequency interaction between inverter and power grid shows various complex characteristics, which

seriously threatens the stable operation of grid connected power system. Qin B et al. presented a unified frequency oscillation method to investigate the oscillation issue in multi VSG grid-connected systems. Grid-connected system model was formulated, and the mechanism behind multi VSG angle frequency oscillation was uncovered [13]. In isolated microgrid, capacity and location distribution in distributed generator are random, resulting in problems such as output and line impedance. Xu H et al. put forward a reactive power sharing approach that relies on virtual capacitors to emulate features of parallel electrical containers at the VSG output end, minimizing sharing errors [14]. Droop control strategy can achieve autonomous power allocation between VSGs, reduce system complexity and enhance reliability. Rasool A et al. proposed a modification to Q-V droop control by adjusting VSG excitation voltage. This adjustment reduced influence of line impedance and rated power in multi VSG systems [15]. In the microgrid, power fluctuations and power grid failures cause system frequency and active power oscillations that seriously threaten its stable operation. Zhang L et al. introduced an enhanced virtual control algorithm using a fuzzy reasoning system. This algorithm was designed for AC microgrid systems [16]. The power distribution of the microgrid and hybrid energy storage system is not uniform enough. Sepehrzad R et al. proposed a control strategy by particle swarm optimization (PSO) and energy management algorithm [17]. In order to provide a grid distributed dynamic model with stable and scalable measurements, Patel S and other scholars proposed a distributed control architecture for distributed energy [18]. The trend of decarbonization has caused excessive pressure on the distribution network. Wang J and other scholars have established an open source environment, elaborated on the active voltage control problem, and successfully promoted MARL algorithm in the real world [19]. The employment of frequency domain identification in broadband technology has gained widespread popularity for analyzing and controlling diverse DC distribution systems. Roinila T and other scholars measured the voltage or current response through the interference of external broadband voltage or current injection through a single converter or system [20].

To sum up, the existing power control distribution strategy still has problems such as uneven distribution and unstable circuit system. This research attempts to add adaptive virtual impedance to the VSG circuit system, establish inertia and resistance characteristics similar to traditional synchronous motors in the circuit system, and analyze the stability of small signals in the circuit system, thus, a distribution control strategy that can always guarantee the stable output power of the circuit system is designed.

2. VSG based parallel power distribution strategy

The appearance of VSG technology can just make up for the shortcomings of low inertia and under damping of traditional inverters, improve power distribution, and stabilize output of electric power. The actual synchronous motor has mechanical and electrical parts. First, the VSG is modeled with this model as a reference, and then the model is subjected to small signal stability analysis. Finally, adaptive virtual inductance further optimizes the model, improve the model distribution efficiency, and simulation experiments are conducted to explore actual power distribution of this model in the process of reactive power and active power output.

2.1 VSG model system construction

VSG technology can be used to imitate the external characteristics of synchronous motor, so that the system itself has damping and inertia. It is mainly to establish corresponding models for the mechanical and electrical parts of the motor, as shown in Figure 1. The stator winding is equivalent to the centralized winding of self-inductance sL and mutual inductance M, and the excitation winding is equivalent to the centralized winding of self-inductance Lf. The mutual inductance between excitation and stator changes with the angular speed of rotor in a sine function curve, where afM, bfM and cfM represent the mutual inductance coefficient, Mf represents the amplitude, r axis represents the magnetic field line of rotor, the rotation direction is counterclockwise, SR represents the resistance of stator group, av, bv, cv represents the output terminal voltage of three phases, and fv represents the voltage of excitation winding.

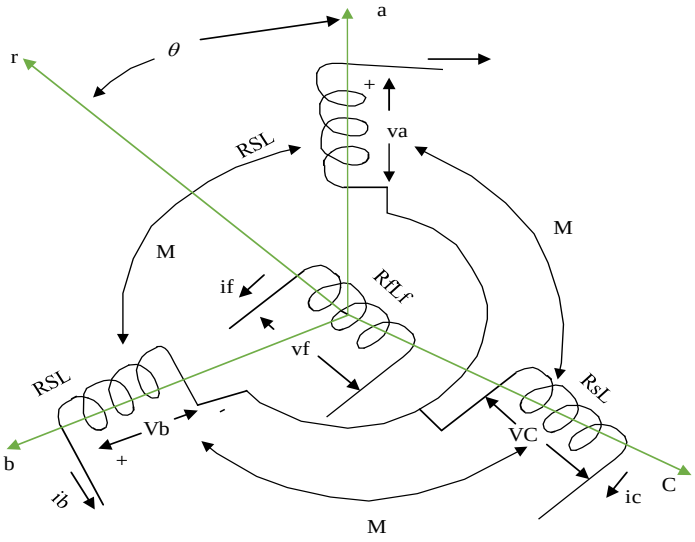

Figure 1. Schematic diagram of ideal three-phase synchronous motor structure

The existing mathematical models with relatively high order can analyze all dynamic electromagnetic processes in detail, but the number of parameters is large, and the VSG algorithm system cannot effectively operate and control. Therefore, simplifying mathematical model of motor as far as possible under the condition that the main parameters of the synchronous motor are taken into account. Under various conditions such as selecting the implicit pole synchronous motor, reducing the order, ignoring the Ni winding, Jiff effect, and the number of pole pairs is 1, corresponding mathematical model is established, as shown in Formula (1):

$$\begin{bmatrix} v_a \\ v_b \\ v_c \end{bmatrix} = \begin{bmatrix} E\cos\theta - L\dfrac{di_a}{dt} - i_a r_a \\ E\cos(\theta - 2\prod/3) - L\dfrac{di_b}{dt} - i_b r_b \\ E\cos(\theta + 2\prod/3) - L\dfrac{di_c}{dt} - i_c r_c \end{bmatrix} \quad (1)$$

In formula (1) and (2), v is the voltage, E is input electromotive force, e is output electromotive force, θ is angle between the electronic windings, L is the length of the excitation winding, and r is the magnetic field line of the rotor.

$$\begin{bmatrix} e_a \\ e_b \\ e_c \end{bmatrix} = \begin{bmatrix} E\cos\theta \\ E\cos(\theta - 2\prod/3) \\ E\cos(\theta + 2\prod/3) \end{bmatrix} \quad (2)$$

According to formula (1) and (2), the general formula of the stator formula is $v = e - L\dfrac{di}{dt} - ri$ (3) to complete the modeling of part of the electrical model.

In addition to the electrical part, there is also a mechanical part of the synchronous motor. The governor of the motor

convert's mechanical energy into electrical energy by adjusting the prime mover valve. At this time, VSG has a short reaction time to energy, which can be controlled sensitively and efficiently, omitting the mechanical movement of the prime mover.

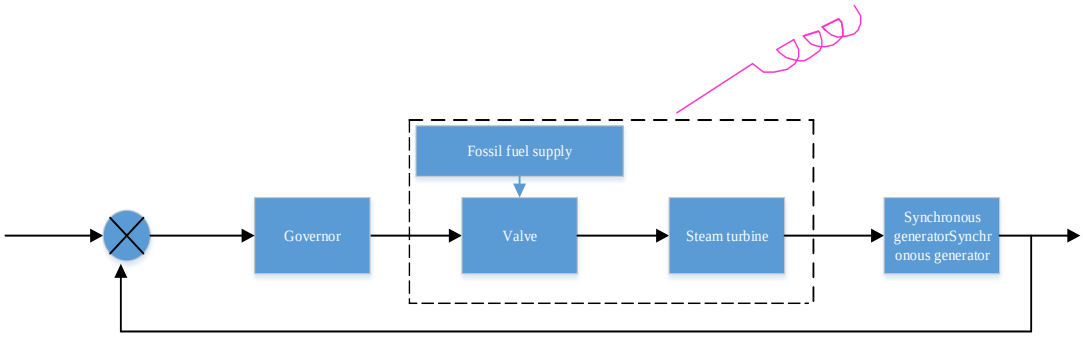

Figure 2. Mechanical Model of Synchronous Motors

Synchronous motor has such a characteristic that when the active power is increased, the motor frequency will be reduced; when the power decreases, the frequency will rise. VSG's control mode for frequency is to simulate such droop characteristics to adjust the frequency of the inverter. This characteristic is shown in the following figure by mathematical formula: w represents the measured output angular frequency, Pref represents the given active power, Pm represents the mechanical power, and k is the coefficient.

$$P_m = P_{\text{ref}} + k_p(w_{ref} - w_{vsg}) \quad (4)$$

Voltage and frequency are common important indicators to judge the level of power quality, and the way of voltage stability is generally by changing reactive power. In the power system, when inductive load with resistance is applied, the output voltage is usually kept constant by adjusting the reactive power and maintaining balance between actual output reactive power; The terminal voltage regulation mode of synchronous generator to generator is that the excitation current is controlled by the excitation system, and then the control system alters the terminal voltage to achieve the desired reactive power output value.

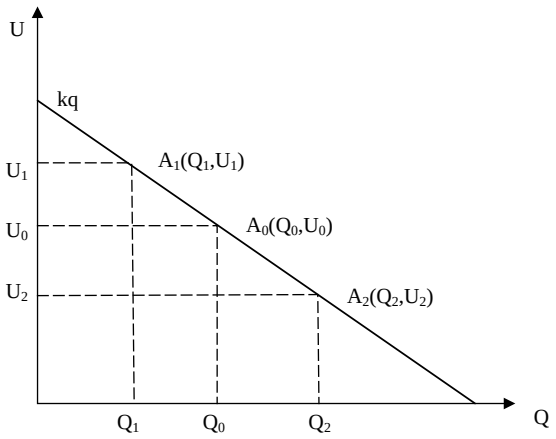

Figure 3. Reactive power voltage regulation characteristics

In a word, the external characteristic of synchronous generator is difference range between reactive voltage and measured reactive power during indirect process of using the excitation system. In the VSG system, if the excitation

current representing reactive power, that is, reactive power and output voltage will retain such regulation characteristics, the regulation characteristics of reactive power and voltage in reactive excitation system are linear.

2.2 VSG parallel system small signal stability

In small signal model of grid connection, the stability of VSG regulation mode is affected by the relevant changes such as active and reactive droop coefficient, damping and moment of inertia. Of course, when it comes to the regulation requirements of PCS, droop control is a frequently utilized method for adjusting the frequency and voltage regulation mode, as it emulates the droop characteristics found in synchronous motors. Droop control formula in frequency domain and voltage is:

$$\begin{cases} w_{vsg} = w_{ref} + k_p(P_{ref} - P_m) \\ U = U_{ref} + k_q(Q_{ref} - Q) \end{cases} \quad (5)$$

Among them, w_{ref} , U_{ref} , P_{ref} and Q_{ref} are generally given values, k_p and k_q in turn represent active and reactive droop coefficients, P_m and Q represent mechanical output power and reactive output power. In this paper, only the relationship between active power and frequency, reactive power and voltage is taken into consideration, thus the rotor inertia link formula including power can be obtained, as shown in Formula (6).

$$\begin{cases} J\dfrac{dw}{dt} = \dfrac{P_m}{w_m} - \dfrac{P_e}{w_m} - D(w_{vsg} - w_{ref}) \\ \dfrac{d\sigma}{dt} = w_{vsg} - w_{ref} \end{cases} \quad (6)$$

Wherein, P_e represents the output excitation power, w_{ref} is the rated angular speed setting value, and w_m is mechanical output angular speed. VSG controller is usually about the rated angular speed, that is $w_m \approx w_{ref}$, the rotor motion formula of droop coefficient can be obtained from this.

$$\begin{cases} J\dfrac{dw}{dt} = \dfrac{P_{ref} - P_e + \dfrac{w_{ref} - w_{vsg}}{k_p}}{w_{ref}} - D(w_{vsg} - w_{ref}) \\ \dfrac{d\theta}{dt} = w_{vsg} - w_{ref} \end{cases} \quad (7)$$

At present, single machine, small power cannot meet the demand for large power in the PCS system, and multiple machines will be used for parallel operation control, as shown in the figure below. In the equivalent circuit diagram of two machines controlled by VSG in parallel, 1, 1, 2, 2U and U are inverters, the voltage at the AC output terminals of 1 # and n #, and 1, 2Z and Z are equivalent output impedance from 1 # and 2 # of inverter to the PCC point respectively; The loadR and loadX voltages are load resistance and inductance. 1U0 is voltage of PCC point; LoadI is output current of load end; 1I and 2I are output currents of inverter 1 # and 2 # respectively.

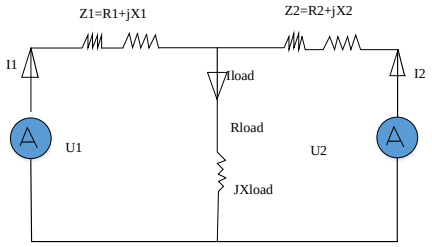

Figure 4. Equivalent circuit diagram of two parallel machines

2.3 VSG parallel power distribution strategy by AVI

In VSG system, the line impedance characteristics cannot be controlled when the probability between each micro source device and the public load is high, which will make the output power distribution of each micro source vary greatly, generate a large number of circulations, and even threaten the stability of the system. As for the on-demand distribution problem caused by VSG parallel power, virtual impedance device is introduced into microgrid parallel system to eliminate the power-coupling problem. When output impedance is resistive at low frequencies or inductive at high frequencies, a certain degree of high-order harmonics will be generated. At this time, if virtual impedance introduced is too large, voltage at PCC point will drop, and the virtual inductance will also distort voltage at PCC point under high-order harmonics, thus reducing the service life of the load equipment. As shown in the figure, for parallel operation of multiple PCS in island mode, all PCS are connected to the load in parallel after LC filtering. The first stage is VSG, PV and DC/DC, and the second stage is PCS. It has been verified that this stage can solve the problem of excessively low battery voltage or large fluctuation during discharge.

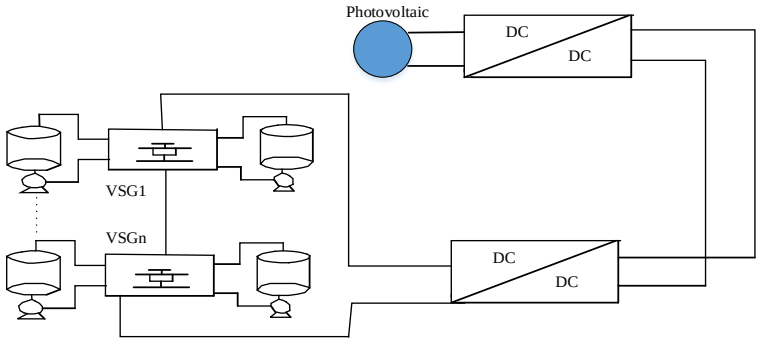

Figure 5. Multi machine parallel topology

Generally, micro sources dominated by photovoltaic or wind power are more vulnerable to natural conditions beyond people's control, which will increase the number of power fluctuations. A larger J is often selected to reduce the fluctuation amplitude, but this will increase the response time of the system, and a larger damping coefficient D is required to reduce angular frequency change. When the system maintains a stable state, a larger damping coefficient will have a certain damping power, which will change the state of the system. One of the preconditions for power distribution based on capacity proportion is that the damping coefficient in the circuit parallel system must increase as inertia and capacity moment increases, and decrease with the decrease. However, in reality, these two variables are difficult to always maintain in the range of the proportional case relationship. Therefore, the adaptive strategy is selected to adjust the power distribution to avoid the above situation.

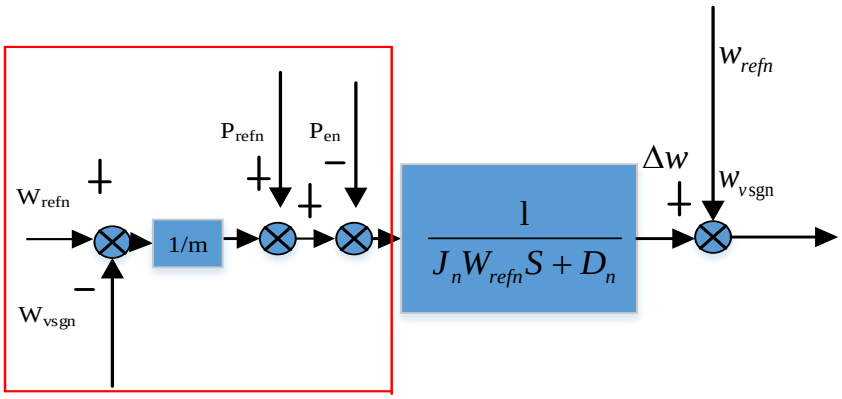

Figure 6. Sag regulation in VSG

When establishing a PCS parallel system, the first PCS will be selected as the reference point, and then the inductance value set by this PCS will be 3 times of the line impedance value. When the flux linkage coefficient and voltage regulation coefficient of PCS in the excitation control system are set to be the same, the difference between the negative terminal voltage of the Nth PCS and the first PCS can be obtained according to the reactive voltage control:

$$\Delta U = U_n^+ - U_1^+ = \left[n_n (U_{ref1} - U_n) + U_{refn} \right] - \left[n_1 (Q_{refn} - Q_1 + U_{ref1} \right] \quad (8)$$

In formula (8), U_n^+ and U_1^+ supplement the change amplitude of output terminal voltage after virtual inductance and impedance, and the reference voltage of all micro source AC output terminals is set to the same, that is $U_{ref1} = U_{refn}$ (9)

Then from formula (8) and (9), (10) can be obtained:

$$\Delta U = U_n^+ - U_1^+ = n_n (Q_{ref1} - Q_n) - n_1 (Q_{refn} - Q_1) \quad (10)$$

According to the power transmission characteristics, the total voltage drop of the first PCS line is:

$$U_1^+ - U_b = \frac{Q1(X_1 + X_{V1})}{U_b} \quad (11)$$

X_{V1} represents the added virtual inductance, then the total voltage on the line of the nth PCS (adding virtual impedance at the output end) drops to:

$$U_n^+ - U_b = \frac{Q_n (X_{vn} + X_n)}{U_b} \quad (12)$$

X_{vn} represents the introduced virtual impedance of the nth PCS. According to formula (11) and (12), the voltage drop between the n-th and the first PCS is:

$$U_n^+ - U_1^+ = \frac{(X_{nv} + X_n)Q_n}{U_b} - \frac{X_1 Q_1}{U_b} \quad (13)$$

The purpose of introducing AVI is to achieve same voltage drop between the nth and the first PCS on the reference impedance, so that there is no circulation in the whole system. From the above formula, (14) can be obtained:

$$n_n(Q_{\text{refn}} - Q_2) - n_1(Q_{ref1} - Q_1) = \frac{(X_{nv} + X_n)}{U_b} - \frac{X_1 Q_1}{U_b} \quad (14)$$

To realize the proportional reactive power distribution, reactive droop coefficient is inversely proportional to the power, and the formula is:

$$\frac{Q_{refn}}{Q_{ref1}} = \frac{n_1}{n_n} = k_n \quad (15)$$

To sum up:

$$X_{vn} = -\left(X_n + \frac{U_b}{k_n} n_1 \right) + \left(n_1 + X_1 \right) \frac{Q_1}{Q_n} \quad (16)$$

In the above formula, Q1, X1, and Ub are real-time transmission of communication mode, so Q1/Qn is a dynamic variable. formula 5.27 shows that when Q1/Qn remains stable, the adaptive virtual impedance value will also remain stable, and no power will be output in proportion to the capacity. In order to reduce the time from Q1/Qn fluctuation to stable state, proportional integral PI is added to adaptive virtual impedance and reactive power control system, also to reduce the fluctuation of AC bus voltage generated during load switching or loading.

3. VSG based parallel power allocation strategy result analysis

After the VSG model is established, simulation experiments are carried out to explore the dynamic response of different moment of inertia and damping coefficient to power distribution; Secondly, small signal influence in the circuit on stability and the improvement of power distribution accuracy by adding adaptive virtual resistance inductance are explored.

3.1 VSG model system construction results

The existence of the damping winding reduces the power system stability, and damping coefficient is included in VSG algorithm to maintain micro source system stability. Simulation experiment results to explore existence impact of damping coefficient on system are shown in the figure. By comparing with the given power, it is found that when the damping coefficient is 60, the response time of lower power is shorter and frequency of oscillation is less; higher power response time is longer, and the frequency of oscillation is more. When the power is small and damping coefficient increases from 60 to 200, the response time and oscillation frequency fluctuate within the same range. At this time, the change of the damping coefficient has little effect on the power. When the power is large, when the

damping coefficient increases from 60 to 200, the response time of the power decreases as coefficient increases, and oscillation frequency decreases in turn. Therefore, when large power changes, larger damping coefficient can better maintain system stability.

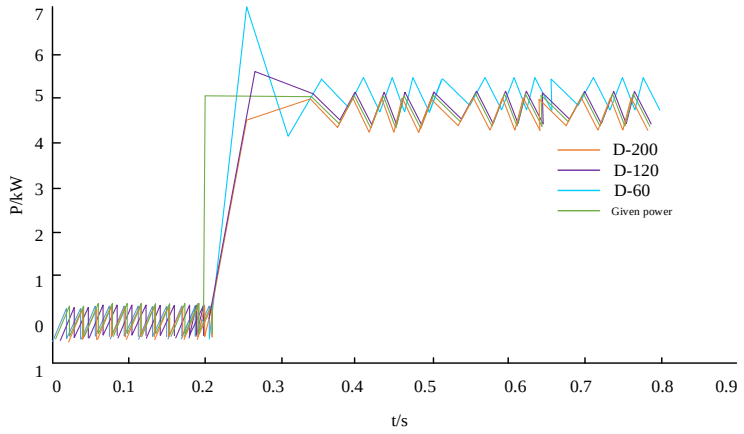

Figure 7. Dynamic response of power under different damping coefficients

The frequency will change with the change of load under different power grid modes. The results of response time analysis of different frequencies through simulation experiments are shown in the figure below. The response time of frequency is different under different moments of inertia. When the moment of inertia is 10, the response time is 0.3 seconds ago, the frequency changes little and remains in a straight line all the time; After 0.3 seconds, the frequency first drops sharply with the increase of time and then tends to be flat. When the moment of inertia is increased from 10 to 15 and 20, the trend of the three curves changing with frequency is similar, but as inertia moment increases, frequency response amplitude will increase, and the stability of the system will be maintained more.

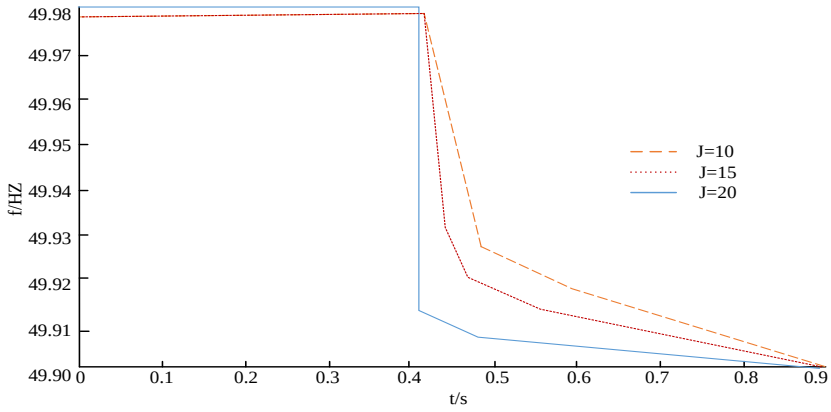

Figure 8. Dynamic response of frequency under different Moment of inertia

In conclusion, the simulation results show that the introduction of damping coefficient into the VSG model system can indeed reduce the impact of other factors on power output and maintain the stability of the system. The greater the damping coefficient is, the better the system stability will be maintained. Influence of the change of inertia moment on power varies greatly with length of response time. In the actual process, selecting the appropriate moment of inertia to maintain system stability is needed.

3.2 VSG parallel system small signal stability analysis

In the given parameters, U=E=220V, W_{ref}=300radls, θ =0.02rad, the equivalent data of filter inductance and VSG synchronous inductance is L=0.318mH. The distribution mode of the characteristic root of the system in the complex plane can be analyzed by using the root track command of matlab in Figure 9.

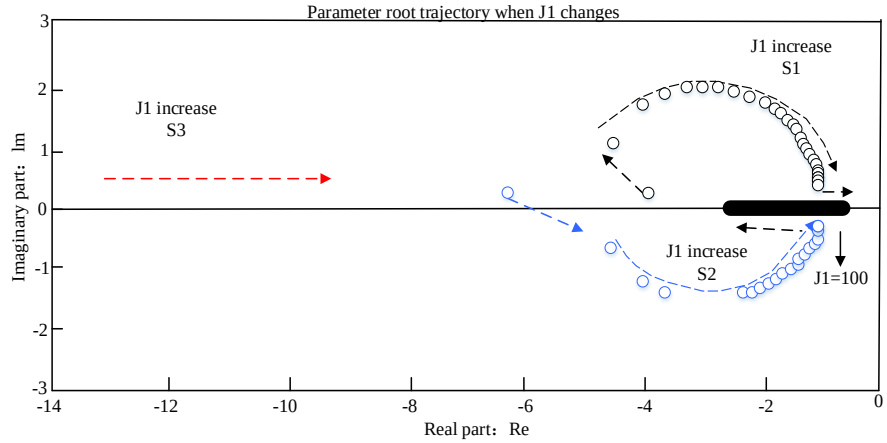

Figure 9. Moment of inertia J1 Root lock when the inertia changes

When setting J2=7, D1=2D1=100, Kw1=2 Kw2=2000, L_W=1.5e-3, J1=7~500, the calculation results show that the system has three characteristic roots, of which S1 and S2 are conjugate complex roots. When J1 is continuously accumulated from 7 to 100, the values of S1 and S2 will be closer to imaginary axis, and VSG algorithm system stability will be reduced; If J1 accumulates from 100 to 500, S1 continues to approach the imaginary axis, even closer to the zero point. System state becomes more and more turbulent, and S2 will be farther and farther away from the imaginary axis, without any intersection with the zero point. However, S2 leaves the zero point more slowly than S1. The change trend of S3 is also close to the imaginary axis with the continuous improvement of J1. However, compared with S1 and S2, the impact of S3 on the system is relatively small and almost negligible. Therefore, the influence of Jd increase on the system changes mainly according to the change trend of S1 and S2, that is, inertia's increase will reduce VSG algorithm system stability.

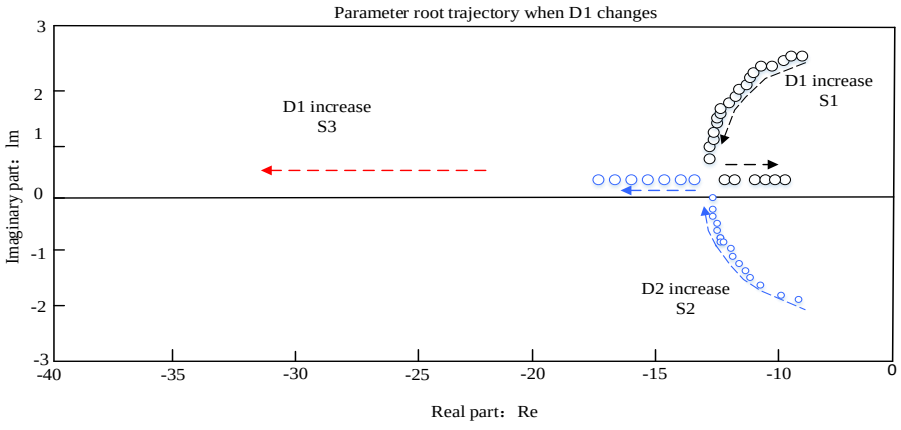

Figure 10. Root trajectory when stamping stakeholder D1 changes

Set each parameter data as J1=8, D1=2, D1=100, Kw1=2, Kw2=2000, Lv=1.5e-3, J2=4~500, and explore change impact of damping coefficient on system stability. Results are shown in Figure 10 above. Similar to inertia influence, system has three different characteristic roots, S1 and S2 are still conjugate complex roots. In process of J2 accumulating from 4 to 315, S1 approaches the imaginary axis from fast to slow speed, and S2 also approaches

the imaginary axis slowly. It can be seen that the impact on system stability decreases slowly; In process of J2 accumulating from 315 to 500, S1 continues to approach the imaginary axis to the vicinity of zero point, and the extreme value is even close to a negative number, which indicates that the state of the system has been extremely unstable and will be in danger, but S1 will leave the imaginary axis and zero point, indicating that the system is temporarily stable at this time. The change trend of S3 is also approaching the virtual axis at a slower speed during the continuous improvement of J2, but its impact on the system is negligible compared with S1 and S2. Therefore, its influence on system will reduce balance of the system with increase of the coefficient.

3.3 VSG parallel power distribution based on adaptive virtual impedance

VSG system without virtual impedance control is simulated, and the impedance ratio and capacity ratio are not inversely proportional. Table 1 shows the results of simulation experiments on output power of different distribution modes. Reactive power output ratio is Q1: Q2=1.36:1, and the output ratio of active power is P1: P2=1.59: 1. Obviously, the ratio is less than twice the size. Moreover, the distributed output reactive power is always within the fluctuation range, with the peak value reaching 8.5k Var, At this time, the output state of power will lead to power coupling. When the line has no virtual impedance, the impedance ratio and capacity ratio are not inversely proportional, which will have a greater impact on the distribution and output of reactive power.

Table 1: Output power of different distribution modes

ive power/Kw	e power/Kw

Add an adaptive virtual inductor to # 1 PCS to keep the impedance ratio and capacity ratio in inverse ratio all the time. Carry out the simulation test under condition 2 in Figure 11. Active power output ratio is P1: P2=2:1, Q1: Q2=2:1, which meets the requirement that the output ratio is double. Compared with the power distribution under condition 1 without AVI, distribution efficiency of this power is greatly improved. After AVI is added, system voltage and current will have an adjustment time in the initial state, about 0.25s, during which the peak current is 6.5A and the maximum difference voltage is 0.32V; after fluctuation regulation, the current of the motor system will be maintained at 0.8A, and the voltage difference at the PCS output terminal is close to 0. This state has met the requirements of circulating current, indicating that the motor system with adaptive virtual impedance can effectively adjust the power distribution.

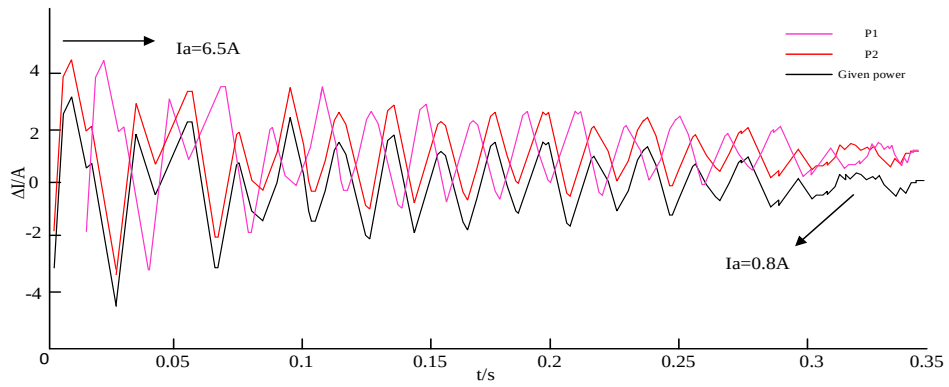

Figure 11. Simulation diagram of working condition 3

To sum up, this simulation experiment compares the distribution of reactive power and active power in the reverse

proportional relationship between impedance and capacity ratio maintained without adding virtual impedance inductance and in the reverse proportional relationship between them maintained with adding AVI in motor system. After adding adaptive virtual impedance, reactive and active power distribution accuracy is significantly improved, which proves the feasibility of this strategy and can make power distribution more stable.

4. Conclusion

To solve unstable power distribution of synchronous motors in actual conditions, a VSG parallel model by AVI is designed. The simulation results showed that both inertia moment and the damping coefficient in VSG affected system stability. As inertia moment and damping coefficient increase, stability of the system decreased. When adaptive virtual impedance was not added, the reactive power distribution ratio was Q1: Q2=1.36:1, and the active power distribution ratio was P1: P2=1.59:1. Neither of them can meet the requirement of 2:1 distribution relationship. In the power output process, the voltage and current fluctuate greatly, and the system was unstable; When AVI was added, active power distribution ratio was P1: P2=2:1, Q1: Q2=2:1, and the distribution relationship between the two met the requirement of 2:1. In the process of power output, the initial voltage difference at the PCS terminal reached the maximum value of 0.32V, and after a short fluctuation of 0.25s, the voltage difference was maintained near 0; The initial peak value of current was 6.5A. After 0.25s fluctuation, the steady-state current of the motor system remained at 0.8A, reaching the basic condition of circulating current. Therefore, the power distribution strategy designed this time can make up for the shortcomings of other strategies in terms of unstable power output and large fluctuation range under the influence of other signals, and the accuracy of this model is higher than other control distribution strategies, which can effectively solve the problem of unstable power distribution of motor system in the actual situation. However, its disadvantage is that the control system is complex, which will consume more resources when applied to the actual situation.

5. Fundings

‘The Fundamental Research Funds for the Central Universities (No. 2021MS123) support the research.

References

[1] C. N. Z. O U, B. Xiong, and H. X. U E, "The role of new energy in carbon neutral petroleum exploration and development," *2021*, vol. 48, no. 2, pp. 480-491.

[2] T. B. Garlet, J. L. D. Ribeiro, and F. de Souza Savian, "Value chain in distributed generation of photovoltaic energy and factors for competitiveness: A systematic review," *Solar Energy*, vol. 21, no. 10, pp. 396-411, 2020.

[3] C. Li, Y. Yang, and T. Dragicevic, "A new perspective for relating virtual inertia with broad ossification of voltage in low energy DC microgrid," *IEEE Trans. Ind. Electron.*, vol. 69, no. 7, pp. 7029-7039, 2021.

[4] M. H. Othman, H. Mokhlis, and M. Mubin, "Progress in control and coordination of energy storage system-based VSG: a review," *IET Renewable Power Generation*, vol. 14, no. 2, pp. 177-187, 2020.

[5] Q. Wu, M. Spiryagin, and C. Cole, "Parallel computing in railway research," *Int. J. Rail Transp.*, vol. 8, no. 2, pp. 111-134, 2020.

[6] C. Zhang and Y. Xu, "Hierarchically coordinated voltage/VAR control of distribution networks using PV inverters," *IEEE Trans. Smart Grid*, vol. 11, no. 4, pp. 2942-2953, 2020.

[7] Z. Li, K. W. Chan, and J. Hu, "Adaptive droop control using adaptive virtual impact for microgrids with variable PV outputs and load demands," *IEEE Trans. Ind. Electron.*, vol. 68, no. 10, pp. 9630-9640, 2020.

[8] X. Liang, C. Andalib Bin Karim, and W. Li, "Adaptive virtual impact based reactive power sharing in virtual synchronous generator controlled microgrids," *IEEE Trans. Ind. Appl.*, vol. 57, no. 1, pp. 46-60, 2020.

[9] A. S. Vijay, N. Party, and S. Doolla, "An adaptive virtual impact control for improving power sharing among inverters in scattered AC microgrids," *IEEE Trans. Smart Grid*, vol. 12, no. 4, pp. 2991-3003, 2021.

[10] M. Ahmed, L. Meegahapola, and A. Vahidnia, "Adaptive virtual impact controller for parallel and radial microgrids with varying X/R ratios," *IEEE Trans. Sustain. Energy*, vol. 13, no. 2, pp. 830-843, 2021.

[11] H. Wu and X. Wang, "Small signal modeling and controller parameters tuning of grid forming VSCs with adaptive virtual impact based current limitation," *IEEE Trans. Power Electron.*, vol. 37, no. 6, pp. 7185-7199, 2021.

[12] O. Babayomi, Z. Li, and Z. Zhang, "Distributed secondary frequency and voltage control of parallel connected VSCs in microgrids: A proactive VSG based solution," *CPSS Trans. Power Electron. Appl.*, vol. 5, no. 4, pp. 342-351, 2020.

[13] B. Qin, Y. Xu, and C. Yuan, "A unified method of frequency ossification characteristic analysis for multi VSG grid connected system," *IEEE Trans. Power Delivery*, vol. 37, no. 1, pp. 279-289, 2021.

[14] H. Xu, X. Zhang, and F. Liu, "A reactive power sharing strategy of VSG based on virtual capacitor algorithm," *IEEE Trans. Ind. Electron.*, vol. 64, no. 9, pp. 7520-7531, 2020.

[15] A. Rasool, X. Yan, and U. Rasool, "Enhanced control strategies of VSG for EV charging station under a low inertia microgrid," *IET Power Electron.*, vol. 13, no. 13, pp. 2895-2904, 2020.

[16] L. Zhang, H. Zheng, and G. Cai, "Power-frequency ossification suppression algorithm for AC microgrid with multiple virtual synchronous generators based on fuzzy input system," *IET Renewable Power Generation*, vol. 16, no. 8, pp. 1589-1601, 2022.

[17] R. Sepehrzad, A. R. Moridi, and M. E. Hassanzadeh, "Intelligent energy management and multi objective power distribution control in hybrid micro grids based on the advanced fuzzy PSO method," *ISA Trans.*, vol. 11, no. 2, pp. 199-213, 2021.

[18] S. Patel, K. Murari, and S. Kamalasadan, "Distributed control of distributed energy resources in active power distribution system for local power balance with optimal spatial clustering," *IEEE Trans. Ind. Appl.*, vol. 58, no. 4, pp. 5395-5408, 2022.

[19] J. Wang, W. Xu, and Y. Gu, "Multi agent information learning for active voltage control on power distribution networks," *Adv. Neural Inf. Process. Syst.*, vol. 34, pp. 3271-3284, 2021.

[20] T. Roinila, H. Abdollahi, and E. Santi, "Frequency domain identification based on pseudorandom sequences in analysis and control of DC power distribution systems: A review," *IEEE Trans. Power Electron.*, vol. 36, no. 4, pp. 3744-3756, 2020.

[21] A. S. Maihulla, I. Yusuf, and S. I. Bala, "Reliability and performance analysis of a series parallel system using Gumbel – Hougaard family copula," *J. Comput. Cooper. Eng.*, vol. 1, no. 2, pp. 74-82, 2022.

[22] X. M. Long, Y. J. Chen, and J. Zhou, "Development of AR experience on electric thermal effect by open framework with simulation based asset and user defined input," *Artif. Intell. Appl.*, vol. 1, no. 1, pp. 52-57, 2023.

[23] Y. Wang, Y. Liu, and W. Feng, "Waste haven transfer and poverty environment trap: Evidence from EU green and low carbon economy," *2023*, vol. 1, no. 1, pp. 41-49.